AD-A107 717 MASSACHUSETTS INST OF TECH CAMBRIDGE DEPT OF MATERIA--ETC F/6 13/8
HEAT SOURCE - MATERIALS INTERACTIONS DURING FUSION WELDING.(U)
APR 81 T W EAGAR, A BLOCK-BOLTEN, C ALLEMAND N00014-80-C-0384

UNCLASSIFIED NL

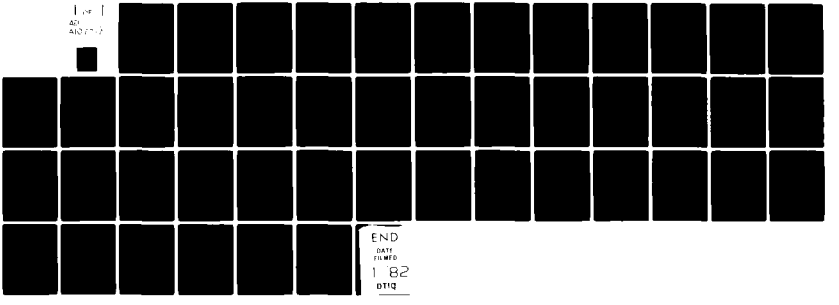

END
DATE FILMED
1 82
DTIC

LEVEL II

12

SECURITY CLASSIFICATION OF THIS PAGE (When Data Entered)

REPORT DOCUMENTATION PAGE

READ INSTRUCTIONS BEFORE COMPLETING FORM

1 REPORT NUMBER	2 GOVT ACCESSION NO	3 RECIPIENT'S CATALOG NUMBER
	AD-A107717	

4 TITLE (and Subtitle)
Heat Source - Materials Interactions During Fusion Welding

5 TYPE OF REPORT & PERIOD COVERED
First Annual Technical Report
April 30, 1981

6 PERFORMING ORG. REPORT NUMBER

7 AUTHOR(s)
A. Block-Bolten, C. Allemand, D. Hardt, J. Katz, C. Huntington and T. W. Eagar

8 CONTRACT OR GRANT NUMBER(s)
N00014-80-C-0384

9 PERFORMING ORGANIZATION NAME AND ADDRESS
Department of Materials Science & Engineering
Massachusetts Institute of Technology
Cambridge, Massachusetts 02139

10 PROGRAM ELEMENT, PROJECT, TASK AREA & WORK UNIT NUMBERS

11 CONTROLLING OFFICE NAME AND ADDRESS
Dr. Bruce MacDonald
Office of Naval Research
800 N. Quincy, Arlington, VA 22217

12 REPORT DATE
April 30, 1981

13 NUMBER OF PAGES
40

14 MONITORING AGENCY NAME & ADDRESS (if different from Controlling Office)

15 SECURITY CLASS. (of this report)
Unclassified

15a DECLASSIFICATION/DOWNGRADING SCHEDULE

16 DISTRIBUTION STATEMENT (of this Report)

Reproduction in whole or in part is permitted for any purposes of the United States Government. Distribution of this document is unlimited.

DTIC
ELECTE
NOV 24 1981
E

17 DISTRIBUTION STATEMENT (of the abstract entered in Block 20, if different from Report)

18 SUPPLEMENTARY NOTES

19 KEY WORDS (Continue on reverse side if necessary and identify by block number)

welding, arc, laser, vapor emission, seamtracking, signal analysis

20 ABSTRACT (Continue on reverse side if necessary and identify by block number)

This report summarizes the first year of progress in studies involving vapor emission from weld pools, design of an infrared microscope for measurement of the weld surface temperature, ultraviolet detection of the weld pool shape, surface reflectivity of aluminum, signal analysis of the weld noise voltage and reflectivity of aluminum by a carbon dioxide laser. The results to date are preliminary.

DD FORM 1473 EDITION OF 1 NOV 65 IS OBSOLETE
S/N 0102-LF-014-6601

SECURITY CLASSIFICATION OF THIS PAGE (When Data Entered)

01 303

DISCLAIMER NOTICE

THIS DOCUMENT IS BEST QUALITY PRACTICABLE. THE COPY FURNISHED TO DTIC CONTAINED A SIGNIFICANT NUMBER OF PAGES WHICH DO NOT REPRODUCE LEGIBLY.

HEAT SOURCE - MATERIAL INTERACTIONS DURING FUSION WELDING

by

T.W. Eagar, A. Block-Bolten, C. Allemand,
D. Hardt, J. Katz and C. Huntington

First Annual Technical Report
Contract N00014-80-C-0384
to
Office of Naval Research
Department of the Navy
Arlington, VA. 22217

Attn: Dr. B. MacDonald

April 30, 1981

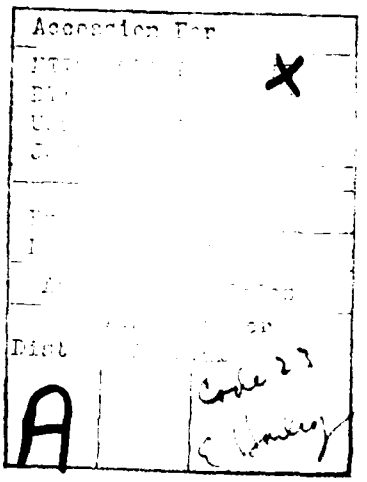

TABLE OF CONTENTS

ABSTRACT

This report summarizes the first year of progress in studies involving vapor emission from weld pools, design of an infrared microscope for measurement of the weld surface temperature, ultrasonic detection of the weld pool shape, surface reflectivity of aluminum, signal analysis of the weld noise voltage and reflectivity of aluminum by a carbon dioxide laser. The results to date are preliminary.

HEAT SOURCE - MATERIAL INTERACTIONS DURING FUSION WELDING

I. INTRODUCTION

This is the first annual technical report of an extensive research program emphasizing welding science. The overall goal of the program is to develop an understanding of the manner in which the alloy composition affects or interacts with the welding process. For example, in arc welding, metal vaporizes from the weld pool which alters the composition, the electrical properties and the thermal properties of the arc plasma. This in turn alters the amount of heat transported to the metal surface, which results in differences in the shape of the weld pool, the weld deposit chemistry and the stability of the welding process. These changes would not be of interest were it not for the fact that previous studies have shown that minor changes in metal composition can cause major changes in the weld deposit. Changes in shielding gas or base metal composition on the order of parts per million can reduce or increase the size of the weld pool by several hundred percent. (1) Such changes cannot be explained by our present understanding of the welding process. In addition, many of the physical phenomena which must be investigated in order to understand the changes noted above may also provide means of controlling the welding process; hence, the work presented here is of more than just academic interest. It is hoped that the results will provide new insight into designing materials which have more uniform weldability and in providing new techniques for monitoring and controlling the welding process. Both of these goals, if achieved, will aid significantly in increasing the use of automation in welding, which in turn should lead to improved productivity throughout many areas in the national economy.

II. ACCOMPLISHMENTS DURING THE FIRST YEAR

In a project of this size, and in experiments of the complexity which are underway, many of the first year accomplishments consist of organizing the personnel and equipment to be used during the project. The effort during the past twelve months has emphasized the following:

A. Equipment Acquisition and Design

1. Optical multichannel analyzer spectrometer
2. Infrared microscope
3. Weld signal analysis
4. Transistor-battery bank

B. Experiments and Preliminary Results

1. Thermodynamic model of vaporization from weld pools
2. Long time spectroscopy
3. Ultrasonic detection of the weld seam
4. Fast Fourier transform analysis of the welding voltage
5. Laser welding of aluminum and aluminum alloys
6. Probes for welding arc analysis

The progress in each of these areas will be described briefly. It should be noted at the outset that the experimental studies are still in progress and the results presented are of a preliminary nature.

A. 1. Optical Multichannel Analyzer (OMA) Spectrometer Equipment

The OMA system represents the single largest equipment purchase of the project. The OMA itself is a two dimensional computer controlled detector (512 x 256 channels) of the vidicon type capable of receiving and storing a series of optical signals of 30 microsecond duration. Other investigators, notably, Mills of Rockwell International (2) and Key of EG & G Idaho (3) have used OMA systems for investigation of welding arc plasmas. Mills performed

a brief series of tests to determine the spatial distribution of Mn metal vapor in the plasma, while Key uses the spectral data to determine the local temperatures in the plasma.

In the present study, the OMA will serve two functions, viz. determination of the temporal and spatial distributions of metal vapor in the welding plasma and detection of the signal from the infrared microscope.

The importance of the temporal and spatial distribution of metal vapors in the arc stems from the fact that these vapors generally have low ionization potentials compared with the shielding gases and hence the metal vapor dominates the electrical properties of the welding arc. In particular, 80 percent of the heat transported to the weld pool is carried by the welding current. Metal vapors from the weld pool may alter the distribution of the weld current, thereby altering the heat flux and the electromagnetically driven fluid flow in the weld pool. It is anticipated that this data will be used as input to a computer model of the arc plasma and weld pool. This model is presently being developed by Prof. J. Szekely of MIT under contract with the U.S. Department of Energy, Basic Energy Sciences.

Although, the OMA represents a very sophisticated optical detector, the optical imaging system used to select the position within the arc plasma is equally critical. During the past year Dr. Charly Allemand has designed a refractive lens and scanning system capable of the following:

1. Detection of major metal elements with a spatial resolution of 0.1 mm and a temporal resolution of 10 milliseconds to one second. Relative concentrations should be measured with a precision of 2 to 10 percent.
2. Rapid changes in metal vapor should be observable with a temporal resolution of 30 microseconds.
3. Minor element concentrations should be observable with a spatial

resolution of 0.1 mm.

Separate optical layouts are needed for each of the three measurements, however the ultraviolet-visible lens is the same for each layout. A brief description of the design specifications is presented in Appendix A. All components have been ordered and received. The six element lens has been tested and found to perform within specification. The entire optical layout for experiment number 1 above, is presently being assembled.

A. 2. Infrared Microscope Equipment

Although infrared microscopes are available commercially, none of these systems are designed to measure temperatures as high as those occurring in the weld pool. During the past year Dr. Allemand has designed a reflective lens which can analyze the spectra from a 20 μm spot on the surface of the weld pool. A brief description of this lens is given in Appendix A.

The mirrors have been machined from solid pyrex glass and are being aluminized. Initial tests indicate that the machining and polishing of the glass has produced mirrors of exceptional quality.

The rationale for development of the high temperature infrared microscope lies in development of an understanding of the heat transport and fluid convection in the weld pool. As noted previously, metal vaporizes from the surface of the weld pool because the local heat flux from the plasma exceeds the heat lost by conduction and convection in the weld pool. The excess heat is lost from the surface by vaporization of metal from the weld pool, much as evaporation of perspiration cools the body on a hot day. Since manganese and chromium in steels and magnesium and zinc in aluminum alloys have higher vapor pressures than the iron or aluminum base metals, these alloying elements are selectively vaporized from the weld pool. Differences in alloy composition alter the vaporization rate from the weld pool which will alter the surface temperature. Measurement of the surface temperature gradients across the weld pool as a

function of alloy composition should aid in understanding the loss of alloying elements from the weld pool. Previous experiments in our laboratory have shown that 0.4% Mn can be lost from submerged arc weld pools by evaporation. (4)

The transistorized welding power supply (described below) will permit measurement of the local surface temperatures by extinguishing the arc and using the high speed capability of the OMA to detect the thermal radiation within less than one millisecond. The thermal time constant of the weld pool is much greater than this. In addition, monitoring the cooling rate at a given location as a function of time will provide some information on the fluid flow behaviour of the weld pool. With the design and receipt of the equipment completed during the past year, experimental data should be forthcoming during the next year.

A. 3. Weld Signal Analysis Equipment

A welding plasma responds to both chemical changes and geometric changes within 50 μsec; hence any disturbance of the arc should cause a change in the welding arc voltage. These changes in voltage alter the heat generated in the plasma, which causes an expansion or contraction of the plasma. These plasma oscillations produce the arc noise which one hears during welding. Since many experienced welders can detect variations in the process by listening to the arc, it can be concluded that the oscillations of interest for process control occur in the audio frequency range. In an attempt to measure these changes a fast fourier transform of the welding noise voltage was needed. Originally, a hard wired FFT analyzer was to be purchased, but it was determined that a computer with appropriate software could perform the same function.

The welding noise voltage was placed on magnetic tape and fed into a computer at the Digital Signal Processing Laboratory at MIT. The results of these tests were encouraging; hence a DEC MINC 11/23 computer was purchased for future signal analysis. This equipment has been received and is operational.

The results of some of the FFT analyses are presented in the experimental section.

A. 4. Transistor-Battery Power Supply Equipment

In order to measure the voltage oscillations of the welding arc, absent of the oscillations in the power supply, a pure DC voltage source is needed. A large battery was acquired early in this project and design of a transistor bank to control the output began; however, in the late fall it was determined that a 20 kW transistor bank would be useful in future studies of gas metal arc droplet formation. Such a transistor bank is beyond the scale of our expertise to construct. Commercial versions are available from Japan and Great Britain at costs exceeding $40,000. Instead, Alexander Kusko, Inc. of Needham Heights, MA was contracted to build a high current D.C. regulator for half this price. The specifications of this D.C. regulator are given in Appendix B. We are confident of Kusko's ability to build this supply as they delivered a 10 kW model to Prof. Matsuchi of the Ocean Engineering Department last summer. By November this 10 kW system had been tuned and proven capable of the specifications. In January we contracted for a 20 kW supply to be delivered in June, 1981. At present all critical components have been received and the regulator is under construction. The delivery date is expected to be met, which will allow us to continue our studies of weld noise voltage sensing and infrared weld pool temperature sensing.

The preceeding four items of experimental equipment have been designed and ordered during the past year. Together they provide a number of unique capabilities for control and analysis of welding arcs. Several of the experimental projects which have been started during the past year will now be described.

B. 1. Thermodynamic Model of Vaporization from the Weld Pool

Since the heat flux to the surface of the arc weld pool is greater than

the heat transported away from the surface by conduction, convection and radiation, the excess heat accumulating on the surface is lost by evaporation. In a pure material, A, the number of moles of metal evaporated is equal to

$$dn_A = \frac{dQ^{xs}}{\Delta H^\circ_{evap}}$$

where dn is the number of moles of metal evaporated

dQ^{xs} is the excess heat transported to the surface which is not removed by radiation, conduction or convection, and

ΔH°_{evap} is the molar heat of evaporation of the metal.

The free energy change associated with the evaporation is

$$\Delta G^\circ = -RT \ln p^\circ_A$$

where p°_A is the standard pressure of metal, A at temperature, T.

In an alloy, the excess heat may result in the evaporation of a number of metals. The overall heat balance becomes

$$dQ^{xs} = \sum_i \Delta H_{evap(i)} \, dn_i$$

where $\Delta H_{evap(i)}$ is the heat of evaporation of species in the alloy and

dn_i is the number of moles of species i.

The free energy change associated with the vaporization of an alloy element is

$$\Delta G_i = \Delta G^\circ_i + RT \ln a_i$$

where a_i is the activity of the element in the alloy.

In order to understand which metal vapors can be expected to dominate the

composition of the welding arc plasma, a series of pressure-temperature diagrams have been developed for iron base alloys. Examples for nickel, manganese, chromium and aluminum are shown in Figures 1 through 4 respectively. Since the weld pool of steel has an average temperature of approximately 2000° C, the dominate metal vapor for any alloy can be estimated by use of these diagrams. For example, Figure 2 indicates that at 2000° C (2273 K) iron and manganese vapor pressures are approximately equal in a low alloy steel containing approximately 0.7 % Mn. In a stainless steel of 18% Cr and 2% Mn, Mn is the dominate species in the vapor. This data is consistent with previous observations in our laboratory that up to 25% of the Mn alloy in a 1.3% Mn carbon steel can be lost by evaporation during submerged arc welding, while the silicon content remained unchanged. (4)

This thermodynamic model can be extended to more complex systems in which compounds form. Examples of the enthalpy-temperature diagrams for titanium-oxygen and titanium-nitrogen systems are shown in Figures 5 and 6. Use of these diagrams permits estimation of the tendency for dissociation or formation of compounds during welding. This information may be important in understanding of flux-metal reactions or compound stability during welding. Previous work in our laboratory has shown that TiN in stainless steels is much less stable in the weld metal than in the base metal, primarily due to a tendency to dissociate at the high temperatures encountered in the weld pool. (5) Further applications of these diagrams to prediction of weld deposit chemistry are being investigated. For example, if one follows the vapor pressure of composition X_{33} (pure titanium) of Figure 5 very carefully, it will be noted that there are several discontinuities in the equilibrium oxygen vapor pressure. It will be noted that the oxygen pressure drops markedly on solidification [illegible] that the combination of the titanium with the oxygen takes place

more readily upon solidification rather than in the liquid phase. In essence, this is not different than noting that precipitation is more prevelant in the solid than in the liquid, however, these diagrams allow one to quantify which precipitates will behave in this manner. In a steel which contains a small fraction of titanium (at a correspondingly low activity) the scale of the vertical axis of Figure 5 is shifted to higher oxygen pressures. By estimating the oxygen potential of the welding shielding gas, and the activity of the alloying element in the weld metal, one can estimate in a quantitative way whether the alloying element will be preferentially oxidized out of the liquid weld metal, whether the oxide will precipitate on solidification or whether it will remain uncombined. Similar plots have been constructed for vanadium-oxygen, chromium-oxygen and zirconium-oxygen systems.

B. Long Time Spectroscopic Facility

In order to measure the rates of metal vaporization from the weld pool a long time spectroscopic facility has been designed, constructed and calibrated by Drs. Andrew Block-Bolten and Charly Allemand. A description of the equipment is presented in Appendix C.

The main purpose of this facility is to study the rate of metal vaporization from a single weld pool over a long period of time e.g. 30 minutes. The relative evaporation rates of three alloying elements is normalized to the vapor of the base metal. In the initial experiments, the rates of Mn, Cr and Al vaporization from steel are being measured using iron vapor as the internal standard. By careful choice of initial steel compositions and analysis of the final weld pool composition, the thermodynamic vaporization models described above may be tested. For example, the model predicts, and others have found, that both Mn and Cr are evaporated from stainless steel weld pools, but the relative vaporization rates cannot be deduced only from

spectroscopic data. By studying the long time change in weld deposit composition and coupling this information with the changes in spectral intensity during the experiment, one can estimate the absolute rate of vapor formation. Such information is essential if a detailed computer model of metal vapor in the plasma is to be performed. As noted previously, Prof. Szekely is developing such a model under DOE sponsorship. This experiment coupled with the spatial distribution of metal vapor as determined with the OMA system should provide valuable input to the model.

B.3. Ultrasonic Detection of the Weld Seam

Prof. David E. Hardt and Mr. Joel Katz of the Department of Mechanical Engineering are studying the possibility of using on-line ultrasonics to monitor the size and shape of the weld pool during the process. They have been reviewing several possible techniques for ultrasonic monitoring of the pool shape. Their progress to date is reported in Appendix D.

B.4. Fast Fourier Transform Analysis of the Welding Voltage

As noted previously, a frequency spectral analysis in the audio range may have potential for detecting changes in the welding process. Several measurements have been made which confirm this hypothesis.

Figure 7a shows the noise voltage of a gas tungsten arc weld on a steel plate. The signal represents the AC ripple on the DC voltage and is remarkably uniform in time. Most of this ripple comes from the rectifiers in the power supply. A very small wind disturbance produces a distortion as shown in Figure 7b. Disturbances of this magnitude can easily be seen with proper signal conditioning.

A more subtle variation in weld noise voltage was produced by melting a one-eighth inch copper wire into a groove on the steel plate and grinding it [illegible]. A cold [illegible] to this "welded" [illegible] voltage signals

as shown in Figure 8a and 8b. Figure 8a represents the AC ripple of the GTA weld without copper contamination and Figure 8b shows the same voltage with copper contamination. Little change can be detected in the real time signal; however Figures 8c and 8d, which are the FFT of Figures 8a and 8b respectively, show that the weld with copper contamination weld has more high frequency noise.

At present it is not known if such signals are reproducible enough for in-process monitoring of the weld quality. With the recent acquisition of a computer in our laboratory, it is hoped that a catalog of signals from welding defects can be established.

B.5. Laser Welding of Aluminum and Aluminum Alloys

A number of previous investigators have found that the coupling of laser energy to aluminum is very poor. There are two possible explanations for this trend, viz. the reflectivity of the solid Al itself is very high, or alternatively, vapor formation blocks the laser radiation from reaching the surface.

Since Al alloys containing highly volatile elements such as Mg and Zn should be more likely to produce plasmas blocking the radiation, a series of tests has been conducted comparing the power absorption of 99.999% Al and 5456 alloy in the electropolished and anodized surface conditions. The power absorption for each alloy as a function of time at low incident power is shown in Figure 9. It will be noted that the surface condition of the pure Al has little effect on the power absorption, while the effect of surface condition with the alloy is very large. These results suggest that at low power inputs, plasma formation is the dominant cause of poor laser coupling on Al. The anodized surface of the 5456 alloy will suppress plasma formation while the electropolished surface presents no barrier to vaporization from the surface. In pure Al, with no strongly vapor forming elements, the effects of the surface condition are slight.

Recent results at higher laser power, which produces significant melting, suggest that plasma formation may be less important. No final conclusions can be drawn from this project at this time, except for the fact that coupling of laser power to the aluminum surface is a function of both alloy composition and surface condition.

B.6. Probes for Welding Arc Analysis

A number of previous investigators of welding have used tungsten probes rotating through the arc to determine the voltage and current distribution in the arc. We have constructed such a probe which spins at 3800 rpm. Most welding investigators have used the maximum voltage as an indication of the center line voltage of the arc, while some others have used the width of the pulse to infer the local current distribution, if only on a relative scale. Upon calibration of the speed of our probe, it was discovered that the probe was indicating an arc width at half maximum voltage of 1.0 cm and a maximum width of 3.2 cm which is clearly not true. Discussions with members of the Physics Department have indicated that use of probes in small, high pressure plasmas such as welding arcs, is not fundamentally sound. Although some data may be obtained, there is no conclusive manner with which to interpret the results. For this reason we have suspended further probe studies and we are reviewing the claims of other investigators who have used these techniques.

III. VISITING COMMITTEE REVIEW

At request of Dr. B.A. MacDonald, a project review was held in November, 1980. The technical reviewers for this project included;

Dr. J. Fox, Idaho National Engineering Laboratory
Prof. D. Olson, Colorado School of Mines
and
Prof. T. [illegible]

The major conclusions of this review were the following:

1. The scope of the program is too broad and should be narrowed
2. The weld noise signal analysis is worthwhile and should be emphasized and
3. The weld pool surface temperature measurement is worthwhile and should not be dropped.

The comments of the reviewers were very helpful, and it is intended during the current year that the following topics will be emphasized:

1. Weld pool surface temperature measurements,
2. Emission spectroscopy of welding arcs, and
3. Weld voltage signal analysis.

It is not so much a matter that the other projects are not worthwhile, but it is deemed that the total project will progress more rapidly if an intensive study of these three topics is undertaken. Nonetheless, the first year has been worthwhile. It was a year of building up of both personnel and equipment. It also permitted exploratory research into a number of topics, the most promising of which will be continued during the next twelve months.

REFERENCES

1. S. Glickstein, WRC Bulletin #226, May 1977

2. G.S. Mills, Welding J., March 1977, p. 93-s.

3. J. Key, EG & G Idaho, Idaho Falls, Idaho, private communication, 1980-81

4. C.S. Chai and T.W. Eagar, to be published in the Welding J.

5. G. Hunter and T.W. Eagar, Met. Trans., 11A, February 1980, p. 213.

Fe-Ni SYSTEM (NEGATIVE DEVIATION)

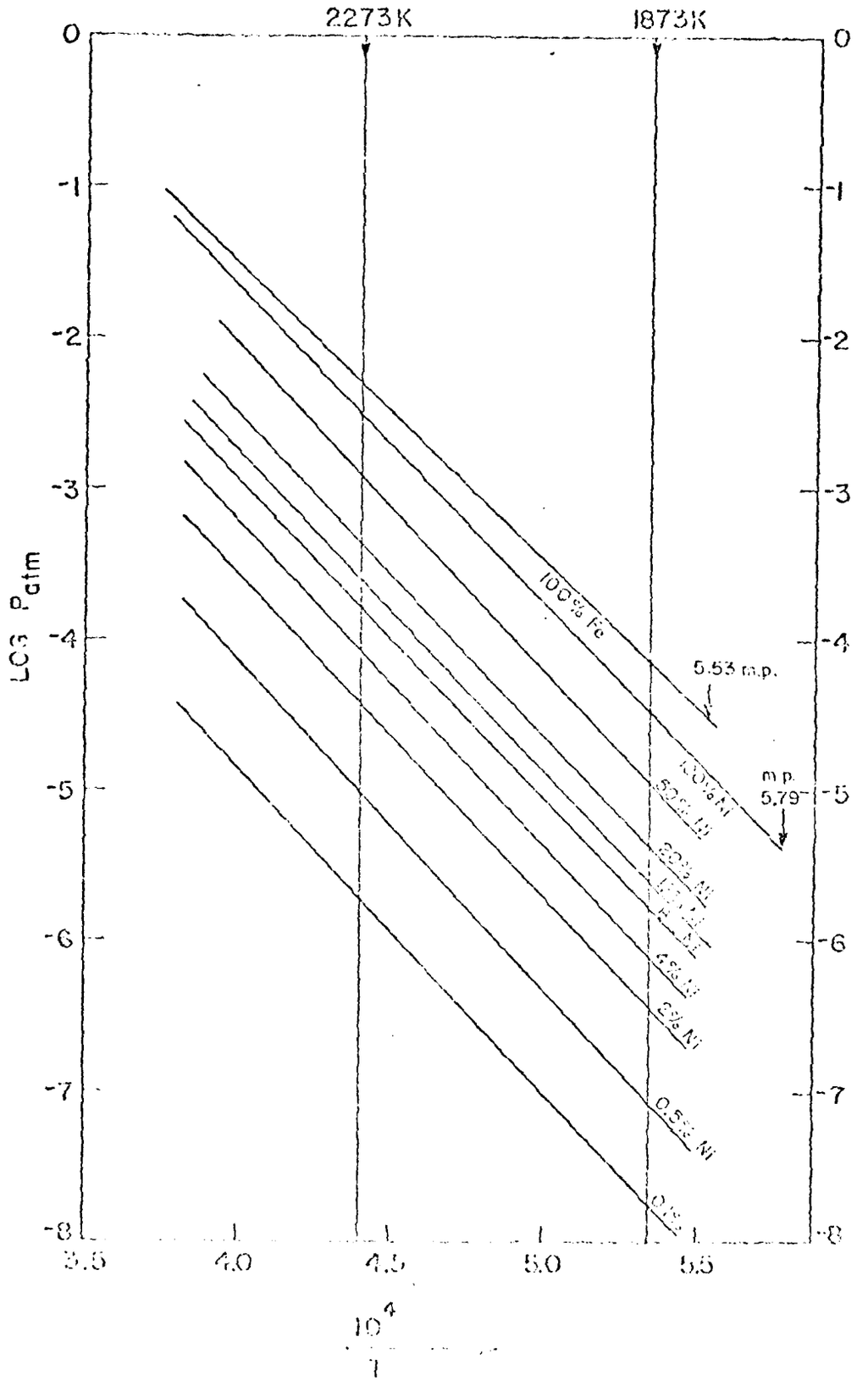

Figure 1

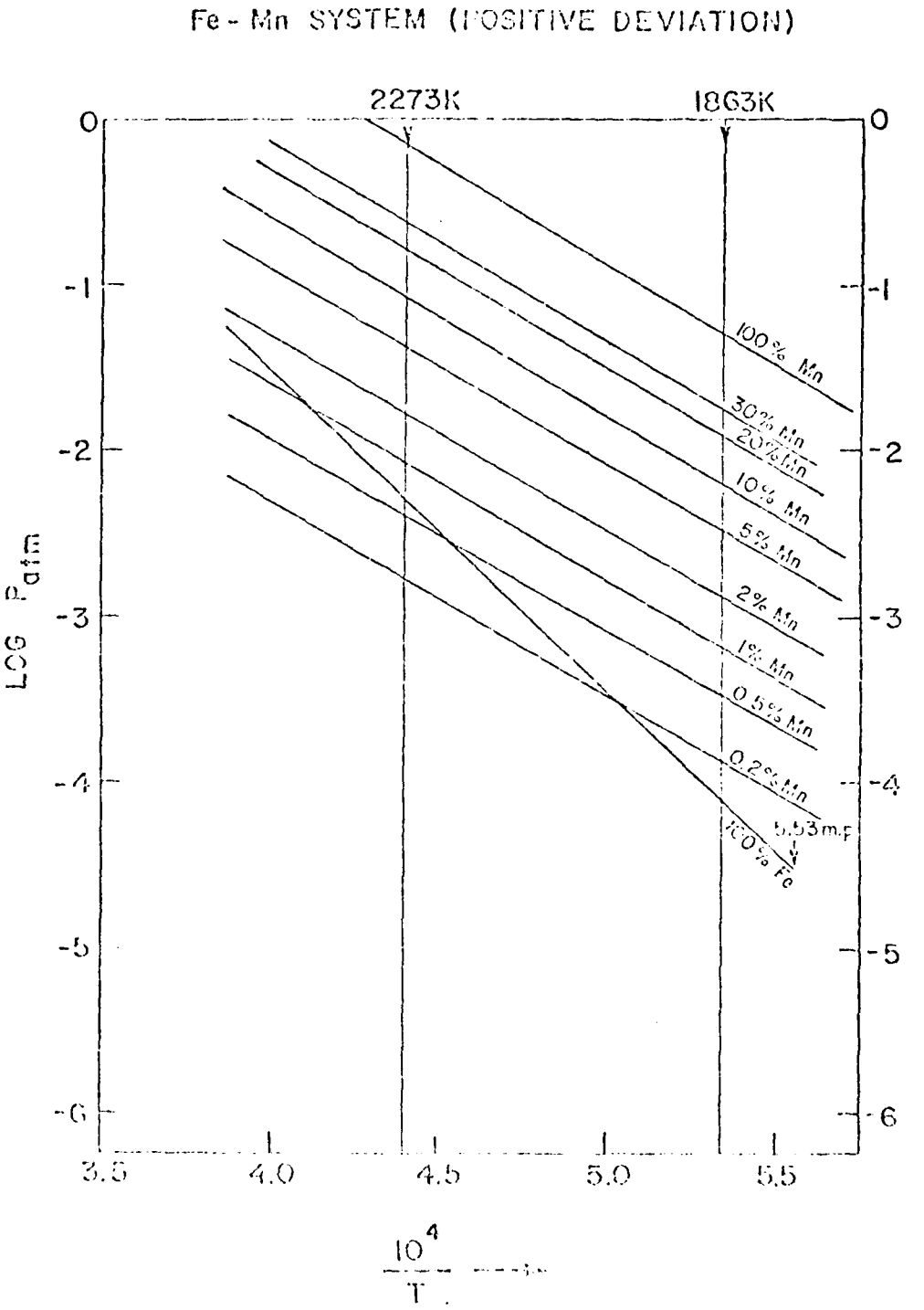
Fe - Mn SYSTEM (POSITIVE DEVIATION)
2273K
1863K
0
-1
-2
-3
-4
-5
-6
LOG P_{atm}
100% Mn
30% Mn
20% Mn
10% Mn
5% Mn
2% Mn
1% Mn
0.5% Mn
0.2% Mn
5.53m.F
100% Fe
3.5
4.0
4.5
5.0
5.5
$\frac{10^4}{T}$ --->

Figure 2

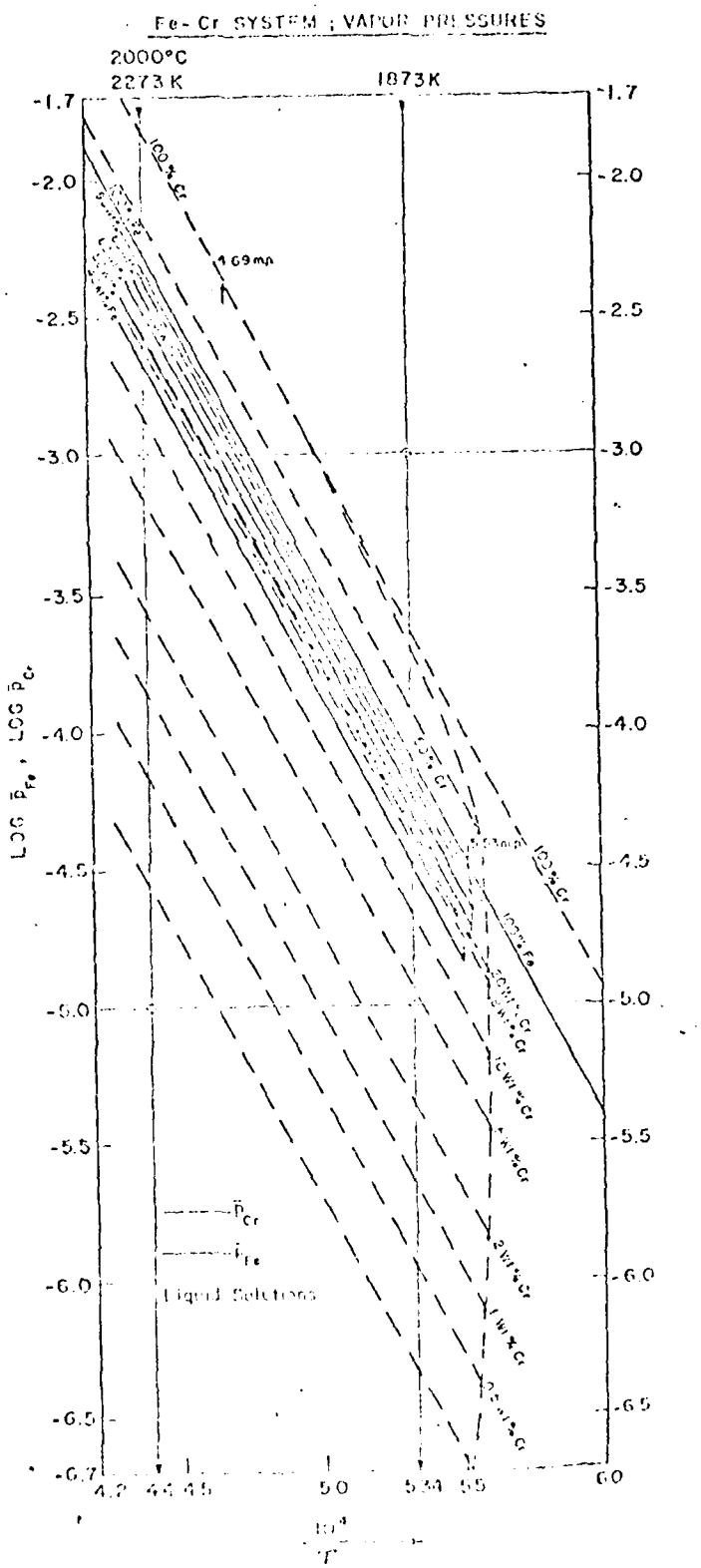
Fe-Cr SYSTEM ; VAPOR PRESSURES
2000°C
2273 K
1873K
-1.7
-2.0
-2.5
-3.0
-3.5
-4.0
-4.5
-5.0
-5.5
-6.0
-6.5
-6.7
LOG $\bar{P}_{Fe}$, LOG $\bar{P}_{Cr}$
100 % Cr
1.69 mm
100 % Fe
$\bar{P}_{Cr}$
$\bar{P}_{Fe}$
Liquid Solutions
4.2
4.4
4.5
5.0
5.34
5.5
6.0
$\frac{10^4}{T}$

Figure 3

Fe-Al SYSTEM (NEGATIVE DEVIATION)

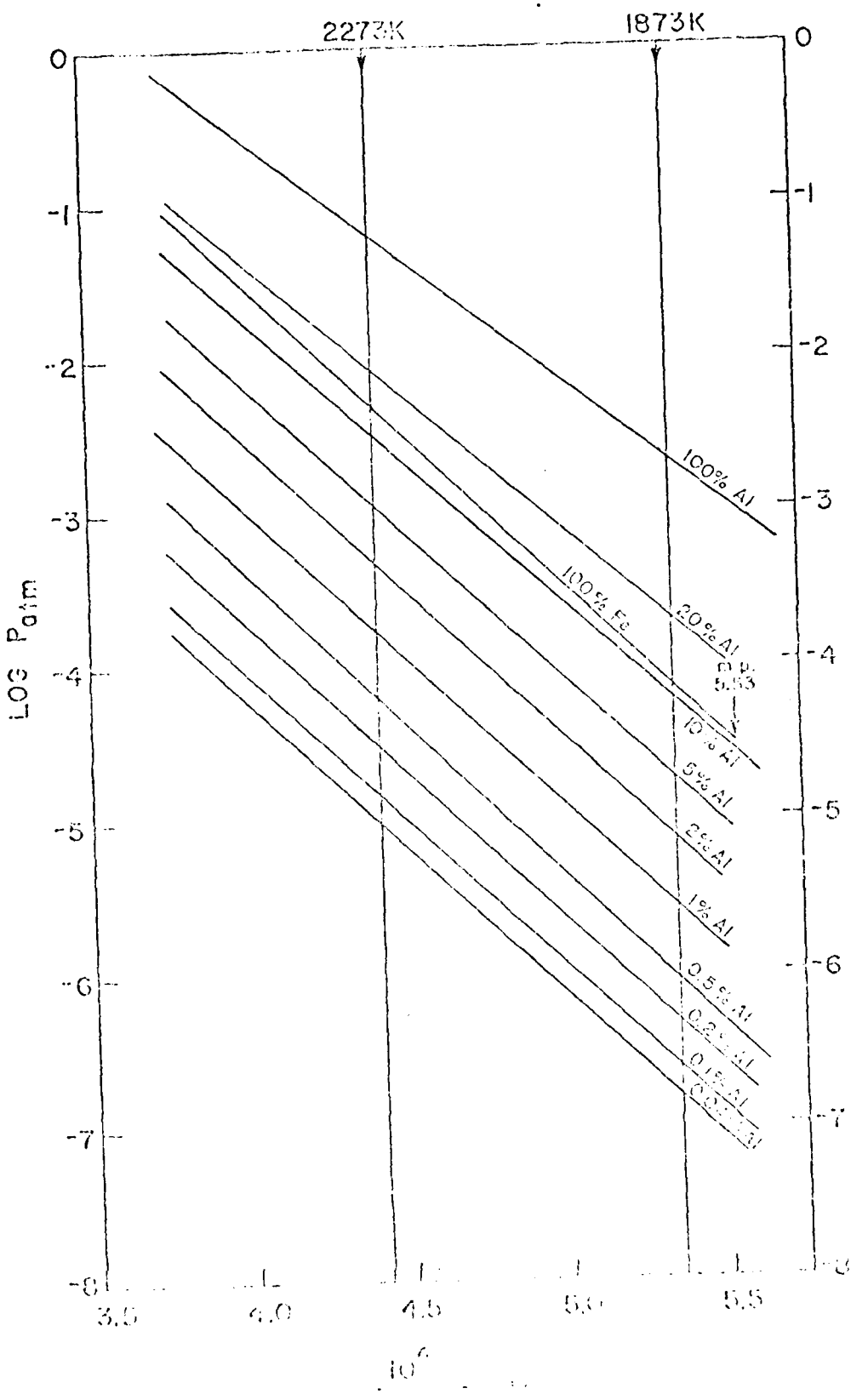

Ti-O SYSTEM

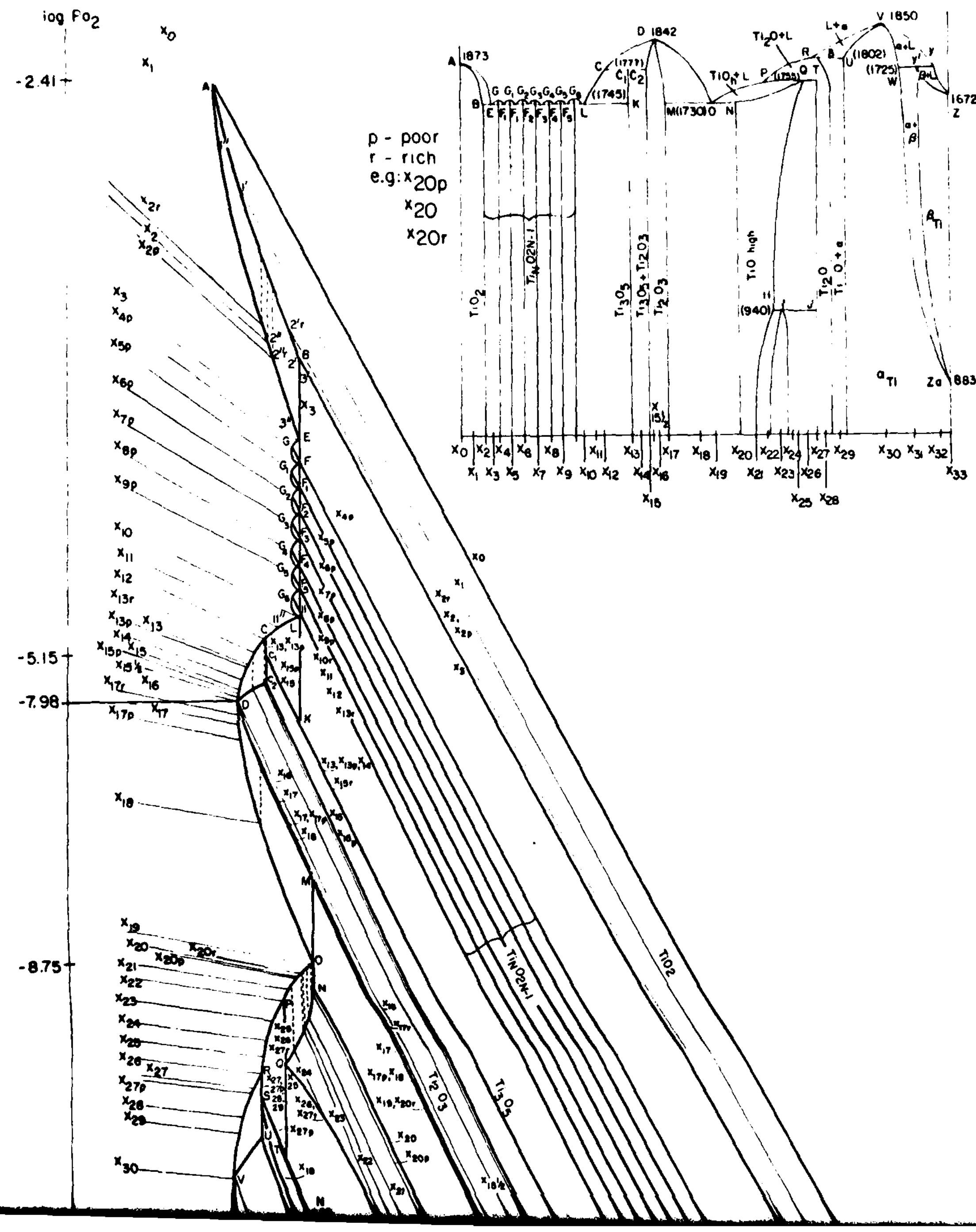

log P_{O_2}
-2.41
-5.15
-7.98
-8.75
p - poor
r - rich
e.g.: X20p
X20
X20r
D 1842
A 1873
V 1850
1672
883
(1745)
(1777)
M(1730)
(1802)
(1725)
(940)
TiO2
TiN O2N-1
Ti3O5
Ti3O5 + Ti2O3
Ti2O3
TiO high
Ti2O
Ti2O+L
TiOh+L
L+α
α+L
α+β
β+L
βTi
αTi
Ti3O5
Ti2O3

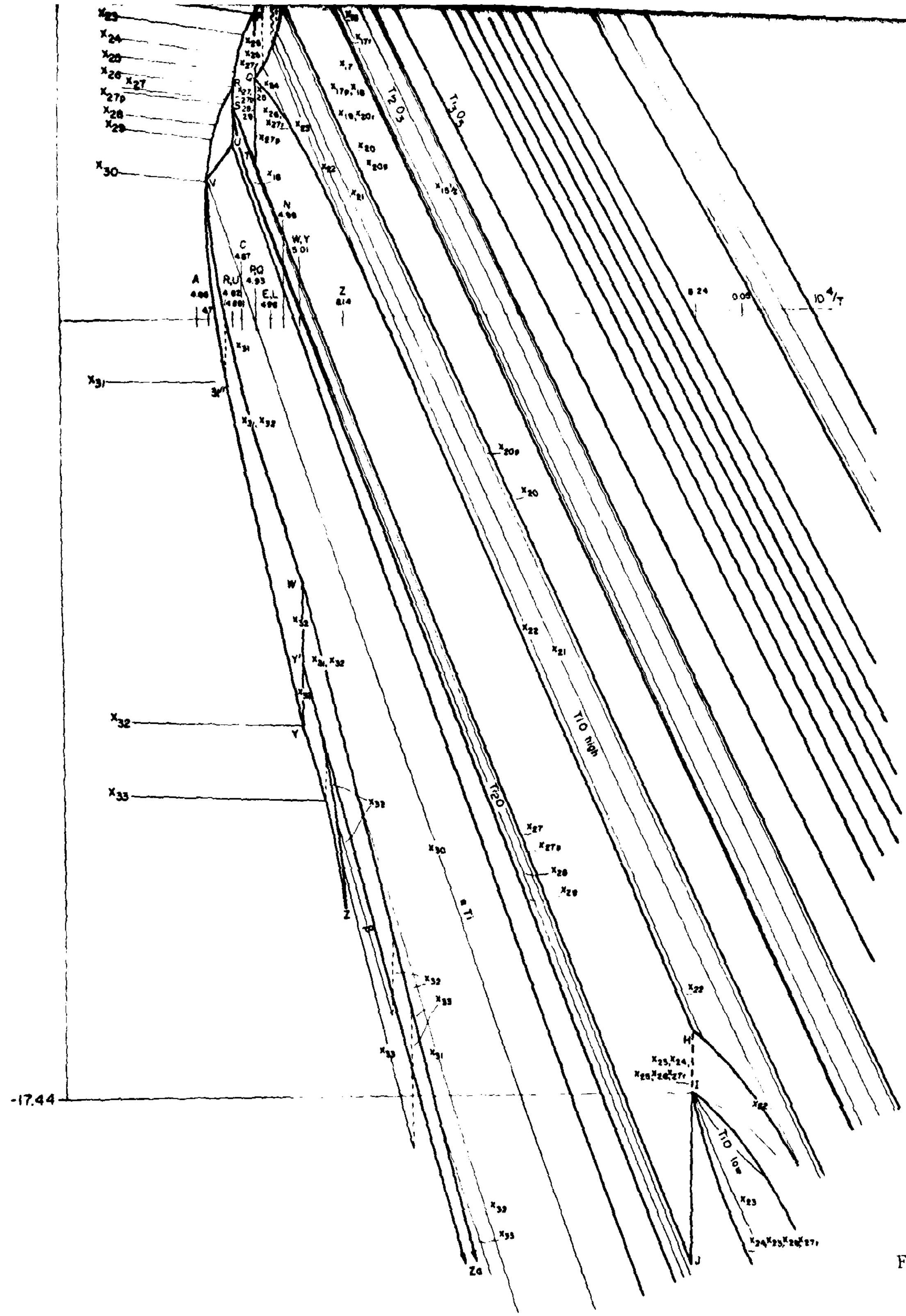

Figure 5

Ti - TiN System

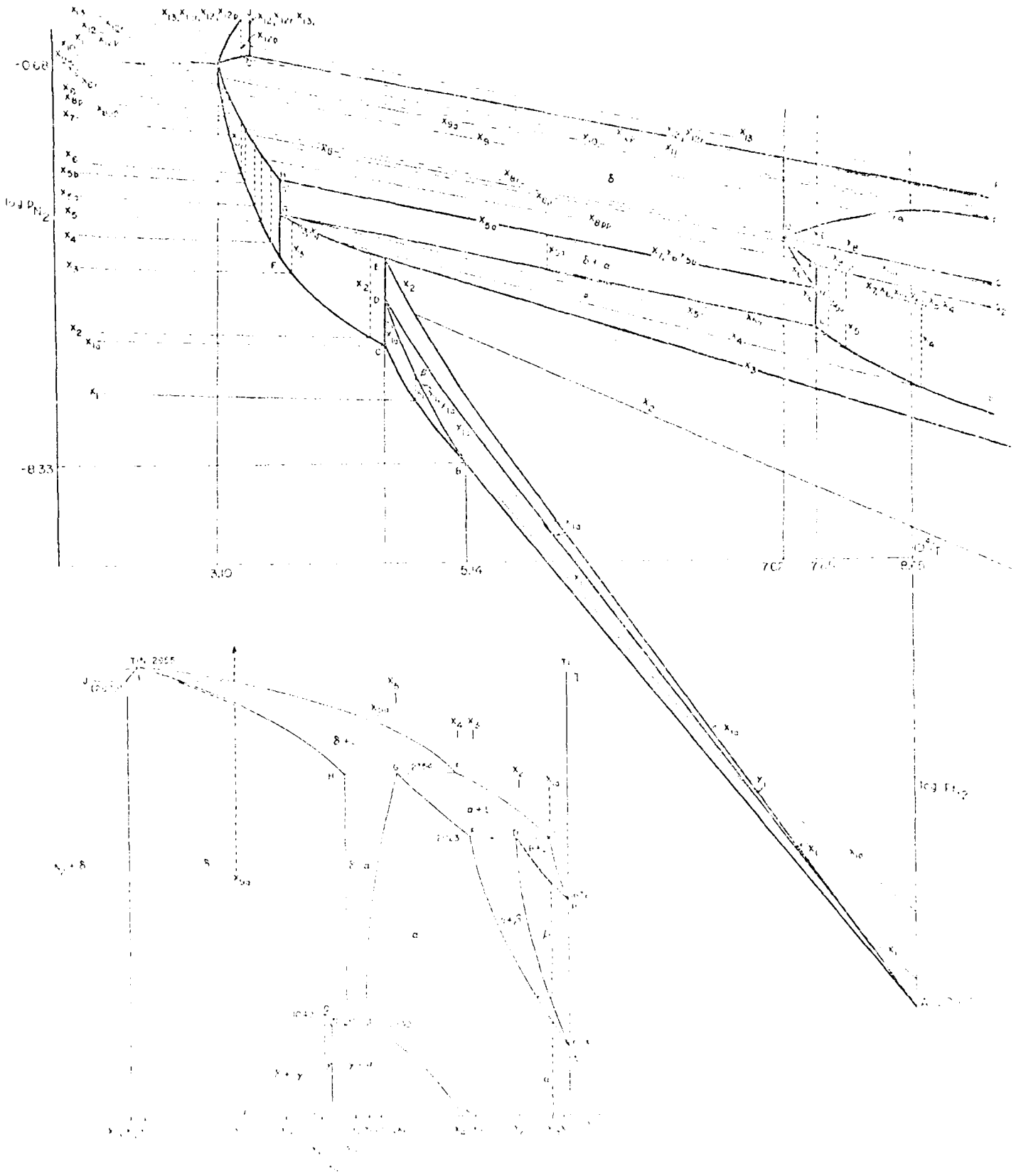

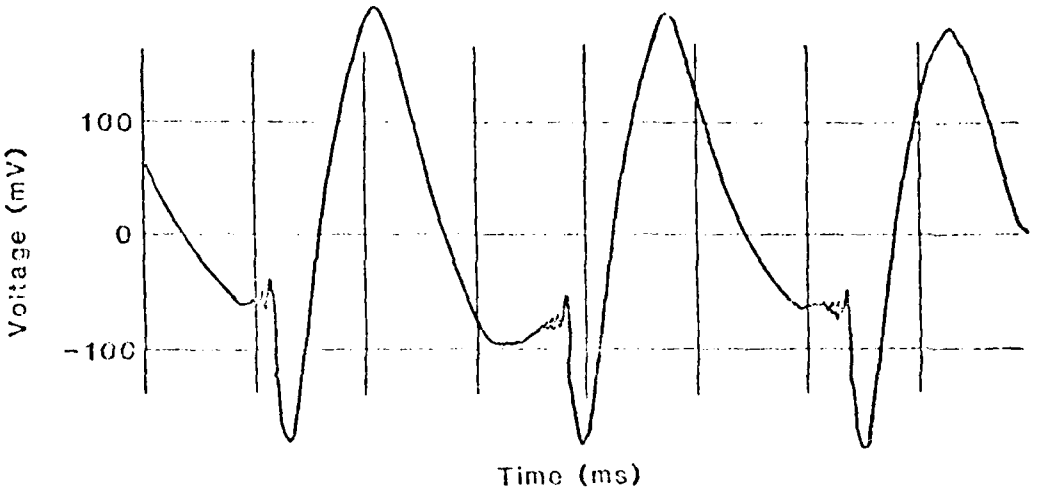

A. Good Weld

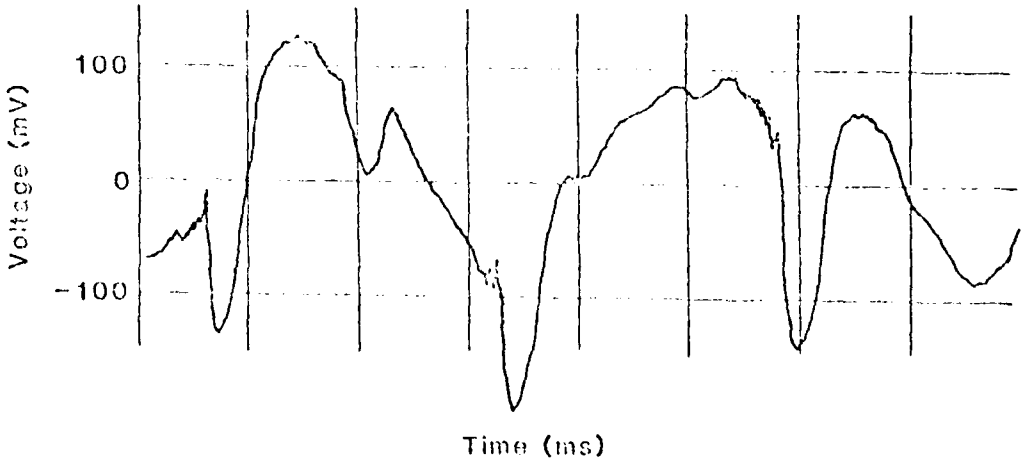

B. Disturbance in Shielding Gas

Figure 7

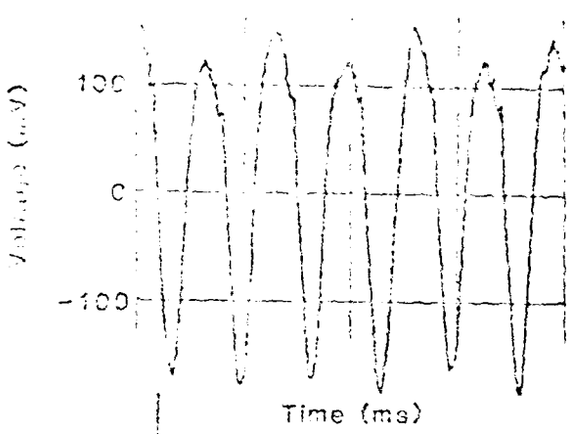

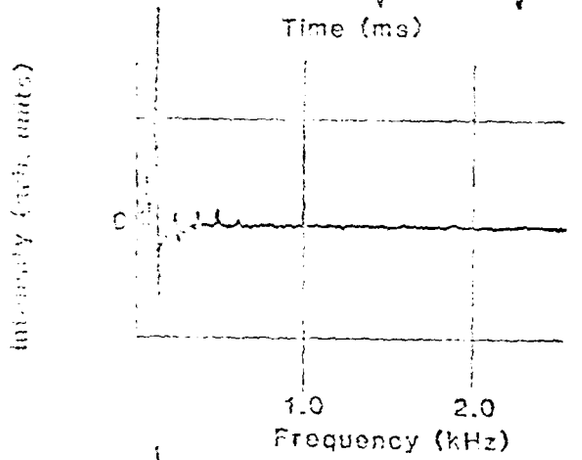

Real

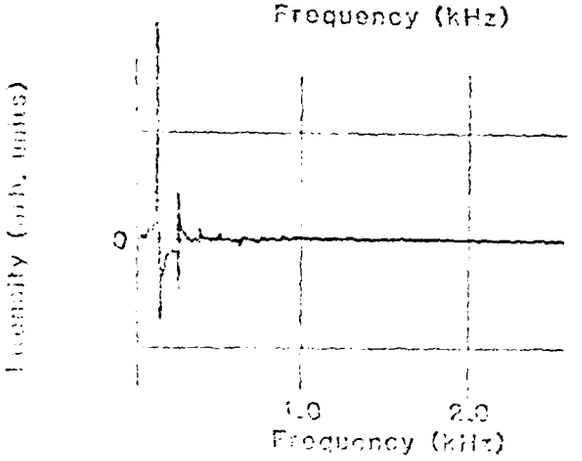

Imaginary

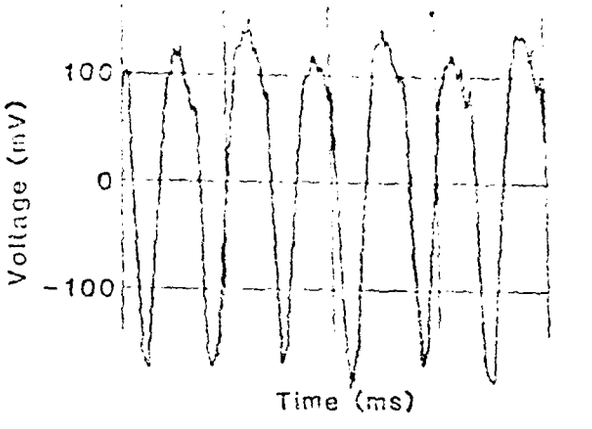

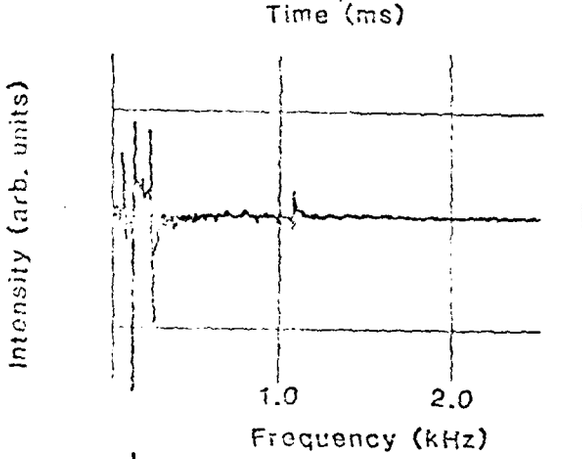

Real

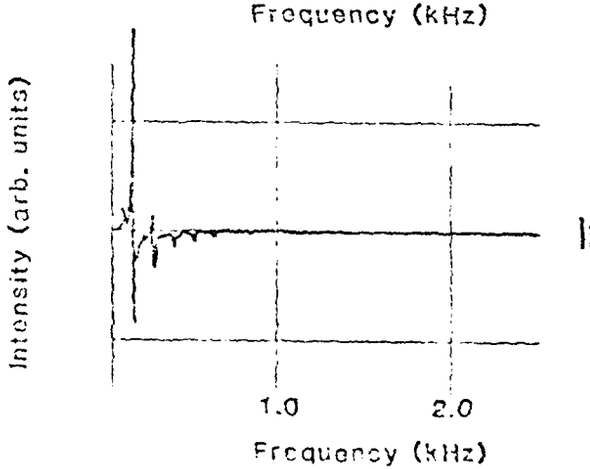

Imaginary

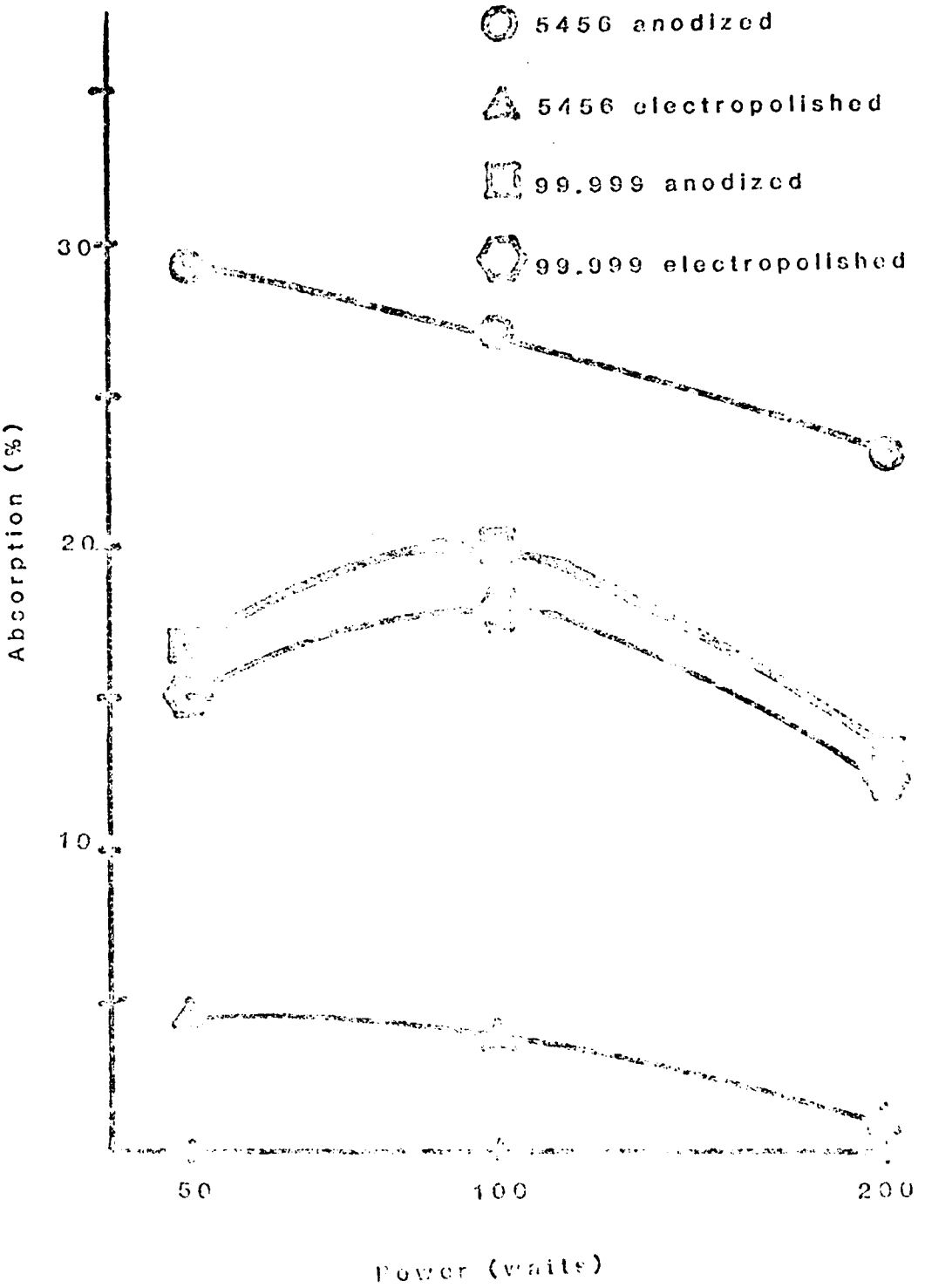
5456 anodized
5456 electropolished
99.999 anodized
99.999 electropolished
30
20
10
Absorption (%)
50
100
200
Power (watts)

Figure 9

APPENDIX A

Design of Infrared and Ultraviolet-Visible for Use with the OMA

Problem Definitions for Experimental Setup

1. The weld puddle surface temperature is to be measured with a precision of ± 10 K with a spatial resolution of 0.1 mm.
2. Major metal elements are to be observed in the welding arc at a spatial resolution of 0.1 mm and their evolution should be followed with a temperal resolution of 10 ms to 1 s. Relative concentrations should be measured with a precision of 2-10%.
3. Rapid changes of metal concentrations should be observed in the arc at a temporal resolution of 30 μs to 10m.
4. Minor element concentrations should be observed in the arc with a spatial resolution of 0.1 mm.

To best approach to these goals, four different optical layouts are needed, each designed to match the specific requirements of one group of measurements. Two different design approaches were followed that are described in the following sections: high precision infrared (IR) and ultraviolet (UV) - visible-based optical trains.

Infrared Optical Train

Puddle surface temperature will be measured using Planck's black body spectral radiant emittance formula. In order to achieve the best possible accuracy spectral radiant emittance will be measured at about 512 different wavelengths in a 250 nm wavelength range, and the Planck curve will be fitted to the experimental results. This will be repeated for several points across the puddle, each

measured circular area having a diameter of 0.1 mm or less.

The effect of the arc emission will be cancelled by momentarily interrupting the arc current. Therefore, it will be necessary to perform each measurement in a short enough time for cooling to be negligible during the measuring time, so that cooling can be measured as a function of time. This will be realized with the use of the OMA system as a detector which is capable of detecting the whole spectrum and sorting the intensity function in a file at times as short as 30 μs.

Calibration of the whole optical train depends critically on the quality of the radiance standard and that of the optical components. In order to avoid the problems usually associated with optical aberrations, we chose the following solutions:

a. to eliminate astigmatism axial viewing only is used. This can be achieved with the use of two directional mirror-scanners.

b. chromatic aberration is eliminated by the use of mirrors.

c. Spherical aberrations are eliminated by the use of off or on-axis aspherics.

In order to model the optical system, Dr. Allemand's exact optical ray-tracing program was used with the MIT-IBM 370 computer. This program was used to estimate the imaging qualities of diverse mirror systems including off-axis parabolas, Cassegrain type mirror combinations based on two spheres or two aspherics, double-cassegrain based on spheres and on aspherics (Figure A1). Finally, a single Cassegrain type combination was chosen based on an elliptical primary and hyperbolical secondary (Figure A2). Its optical quality may be estimated from a simplified spot diagram shown in Figure A3 and obtained from our ray-tracing program. On the left side of Figure A3, a 5 mm dia. source area is represented by 19 sampling points distributed on circles. The images of three of these source points are characterized by the impact points of traced

rays (19 for each source point) on the image plane. The largest extent of the image is obtained for a source on the outermost circle. This spot covers about 12 μm, confortably smaller than the required 0.1 mm. On axis of course, the model shows a perfect image.

The shole optical train, comprising this cassegrain type mirror, scanners and a spectrograph is being mounted on a sturdy commercial optical bench.

The parabolic and hyperbolic mirrors have been ordered and were received in April 1981.

UV-Visible Optical Trains

Spectroscopic observations will not require as aberration free an optical system as the infrared microscope, unless a good spatial resolution is required as would be the case for arc temperature measurements based two line intensities and requiring an Abel inversion. The IR mirror optics can also be used for spectroscopic determinations, but since it cannot be diaphragmed down below the solid angle intercepted by its secondary mirror, it will be useless when very small aperture angles are to be used. Therefore, a symmetrical double-triplet lens was designed out of quartz and calcium fluoride (Figure A4). This lens can be used at wavelengths as low as 240 nm with very small abberation. Figure A5 is a representation of the spectral spherochromaticity of that system computed with Dr. Allemand's ray-tracing program. On the vertical axis is represented the height in mm of the impact point of the considered ray on the entrance pupil, and on the horizontal axis is the intersection (focus) of that ray with the axis, also in mm. The spherochromaticity for wavelengths from 210 to 587 nm is shown. As can be seen for rays on a diameter of 60 mm, the focus will remain on a 1 mm segment of the axis for wavelengths between 240 and 587 nm.

This system will be used in optical layouts where chromatic and spherical abberations have to be minimized. Where these two requirements can be relaxed, we also have the possibility of using single lenses.

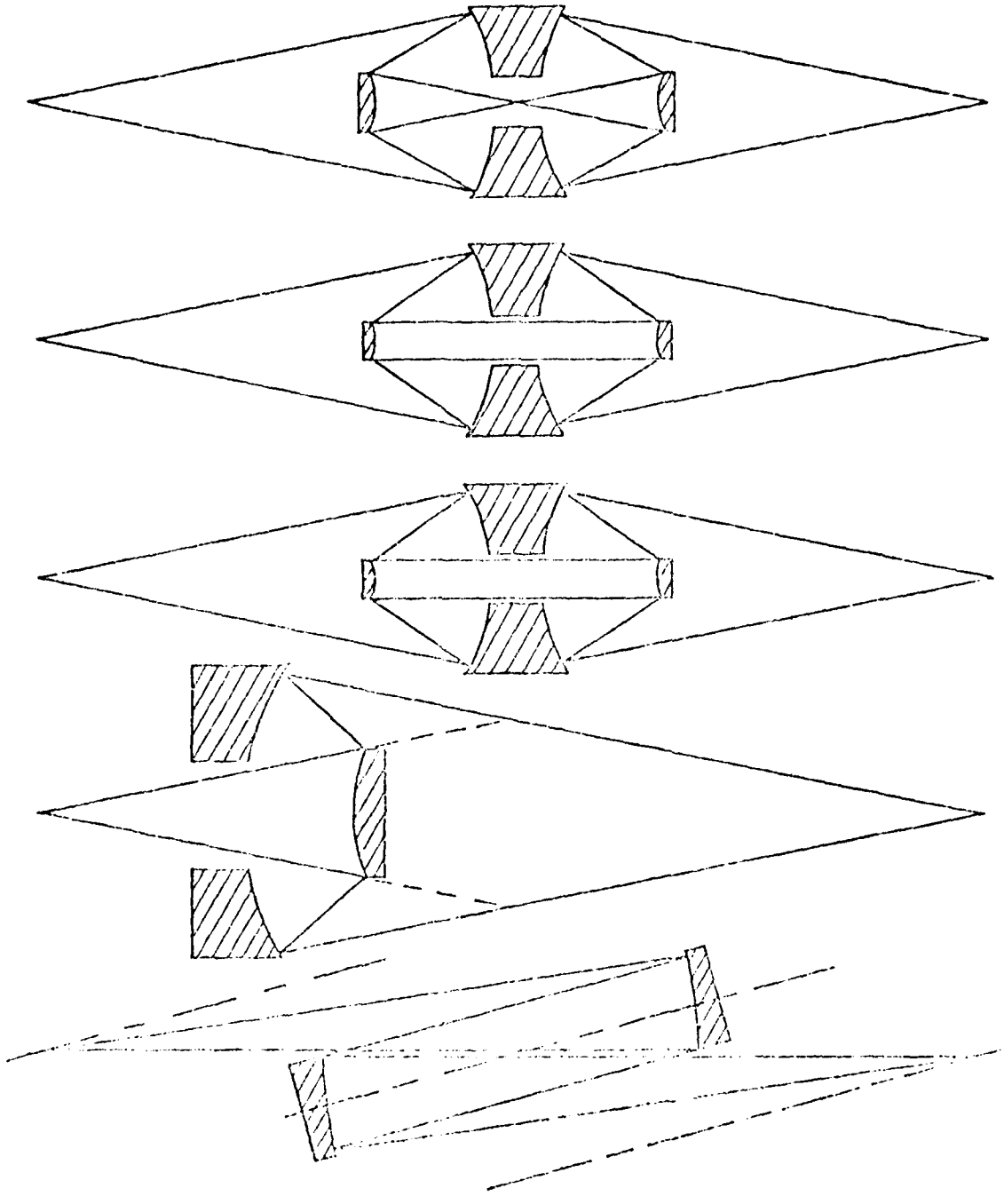

Figure A-1

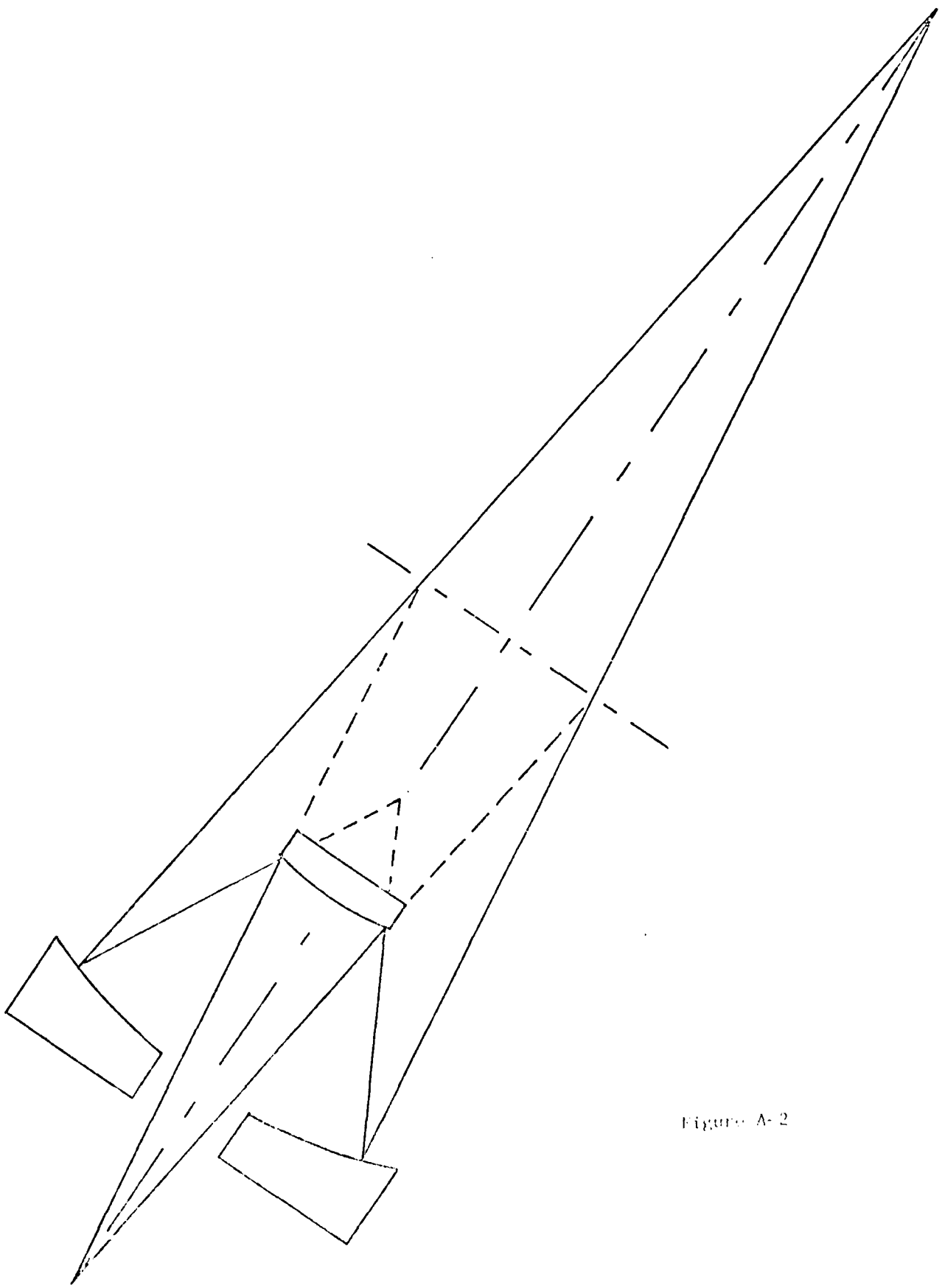

Figure A-2

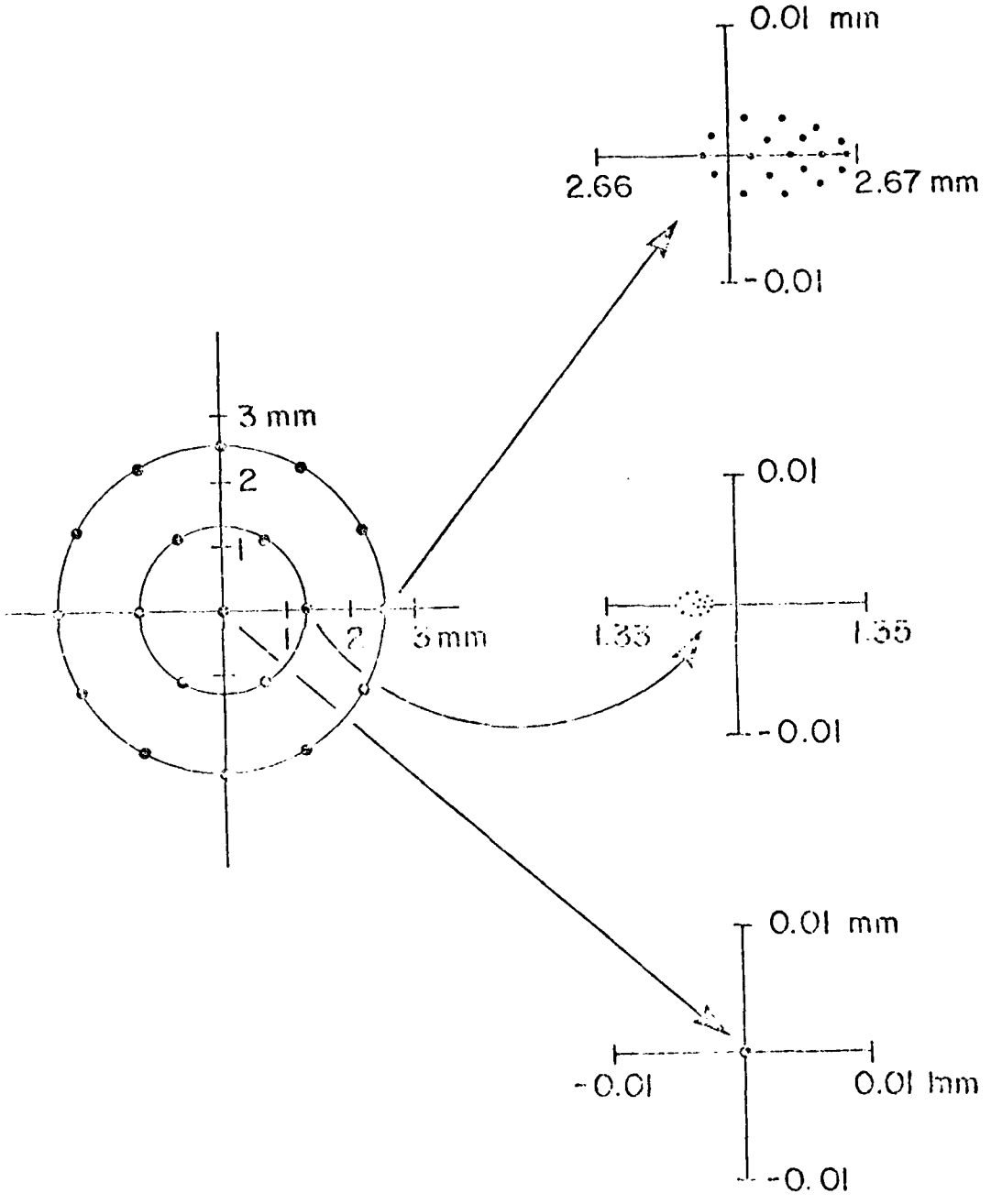
0.01 mm
2.66
2.67 mm
-0.01
3 mm
2
1
1
2
3mm
0.01
1.33
1.35
-0.01
0.01 mm
-0.01
0.01 mm
-0.01

Figure 2.3

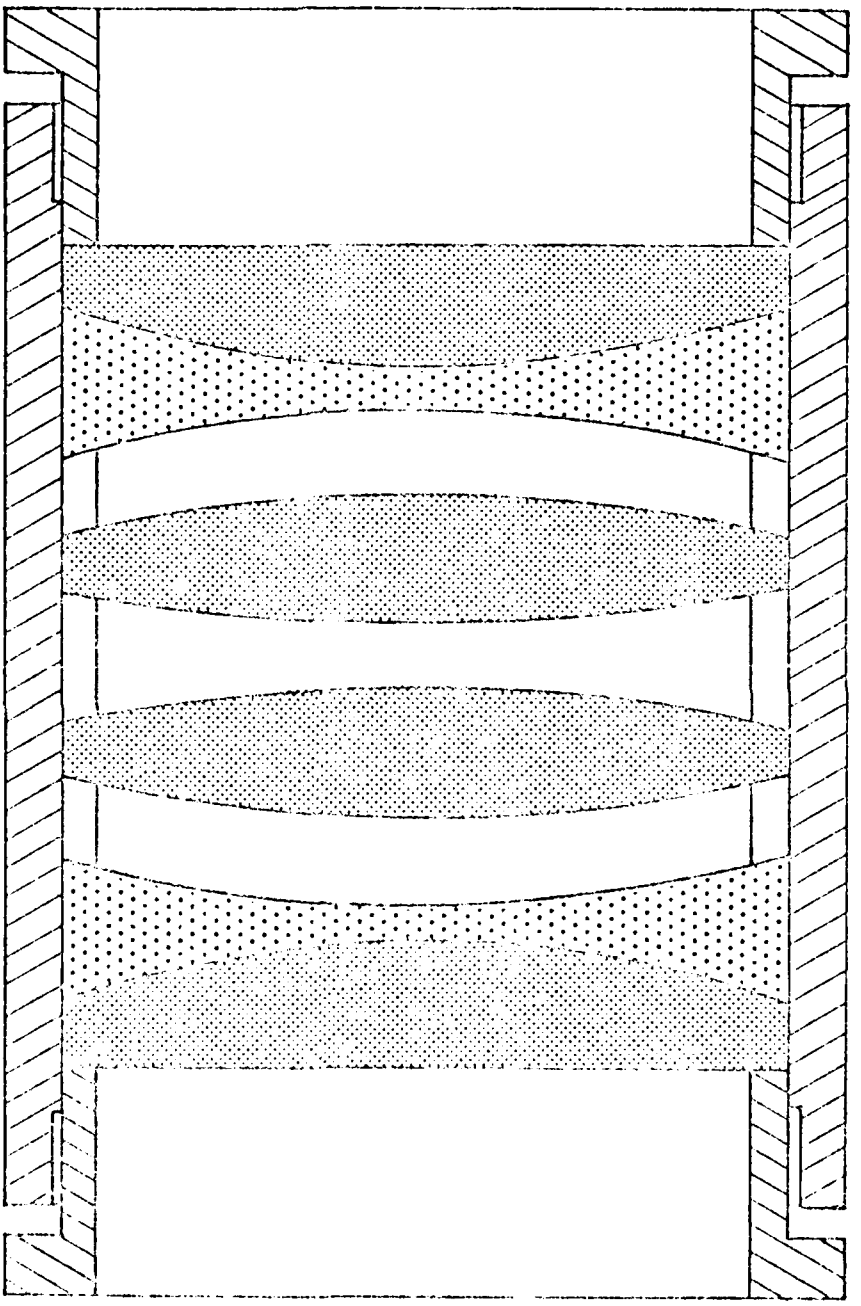

Figure A-4

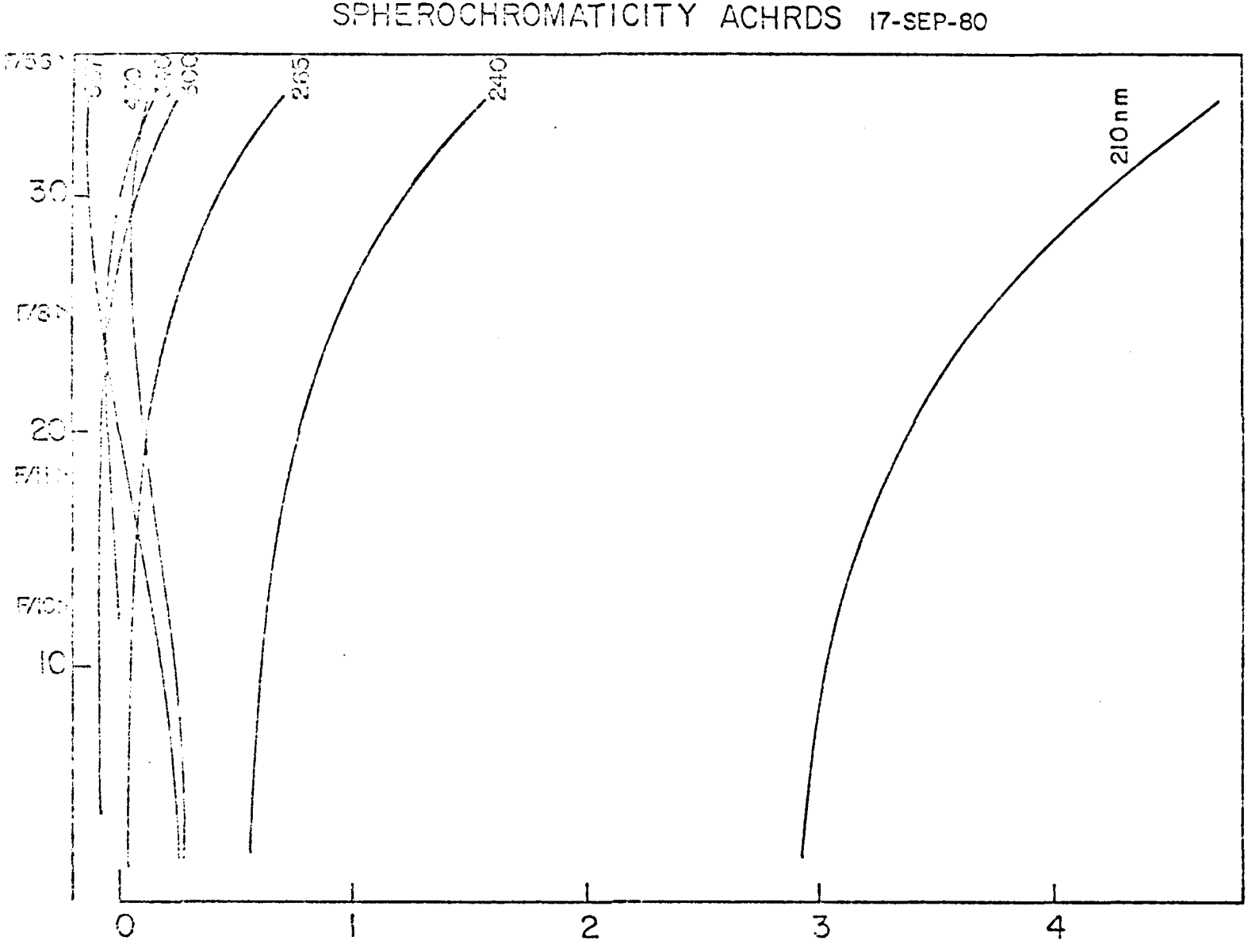
SPHEROCHROMATICITY ACHRDS 17-SEP-80
265
240
210nm
30
20
10
0
1
2
3
4

Figure A-1

APPENDIX B

High Current DC Regulator

Specifications

The mechanical and electrical specifications for the Current Regulator are as follows:

1. Inputs: 0-80 V dc at 0-1000 A. 120 V ac at 3 A.
2. Output: 0-1000 A dc for a resistive load.
3. Output current is continuously adjustable from 0-600 A.
4. Front panel control for adjusting the output current is provided.
5. Front panel metering of output voltage and output current is provided.
6. The regulator will be constructed in a standard 19" relay rack cabinet. Cabinet to be supplied by MIT.
7. Forced air and water cooling are used. Water requirements do not exceed 5 GPM with inlet pressure not exceeding 25 psig. Open cycle water cooling is used.
8. Appropriate high current dc terminals for input and output are conveniently located.
9. Automatic shutdown is provided under the following conditions:
   a. loss of water flow rate
   b. high heat sink temperatures
10. Output signals for monitoring output voltage and output current are provided.
11. External current control, by means of external current signal, is provided. External input is 0 -10 V full scale with input impedance greater than 1 MΩ and accuracy of 0.1% of full scale.

12. The output current response to a step change in the external current reference signal will have the following characteristics with respect to a 0.1 Ω resistive load.
    a. The output current will settle to within 1.0% of full scale within 250 μs over the entire operating range.
    b. The output current response will have less than 10% overshoot over the entire operating range.
    c. Items a and b above will be met within the restriction implied by the open circuit supply voltage.
13. The supply is suitable for use with certain types of RF arc starting equipment.
14. The supply will deliver 600 A continuously at an output voltage of 25-60 V dc with an input voltage of 80 V dc or less and specified water flow.
15. The thermal design and overload protection of the supply are designed for 600 A rms.
16. The supply will continuously deliver arbitrary current waveshapes of 600 A rms with peak currents not exceeding 1000 A.
17. The supply will deliver full current into a short circuit for periods of 5 s or less.

APPENDIX C

Long Time Spectroscopic Measurements

The extended time spectroscopy of the vapor phase above the weld pool permits an estimation of the absolute rates of metal vaporization into the welding plasma, as well as determination of the share of vapor concentrations of individual alloying elements. A mass balance of the evaporating elements, from the start to the finish of the experiment will be helpful in determining the selectivity of evaporation in different steels and alloys. It will also permit extrapolation of the process to the short time encountered in welding. In order to reach this goal, experimental equipment has been built consisting of a three meter CEC Emission Spectrometer obtained from surplus, adapted with new electronics. A watercooled welding-turntable has been fitted inside a watercooled chamber, as presented in Figure C-1. An argon tent has been built around the chamber. The turntable is driven by a variable speed motor. The detector consists of a Fluke power supply providing high voltage to the photomultipliers, of four Keithley picoampmeters which read signals from iron and from three other photomultipliers; of three dividers providing ratios of signals; of three multimeters for monitoring the experiment and of two two-channel recorders reading, and recording the spectral ratios of the three alloying elements as well as the pure iron signal. The iron signal is the internal standard as the activity and the partial pressure of iron ($\bar{P}_{Fe}$) is hardly affected by the alloying elements during the test. Between the picoampmeters and dividers three kinds of filters have been installed: filters a and b eliminate the high frequency weld start signal which was found to be composed of two separate frequencies, and filter c eliminates the 60 cycle vibrations.

Although over 50 channels (elements) are available on the CEC Spectrometer, the difficult alignment allows for no more than four channels to be used simultaneously. Hence, it is possible to measure elements other than Fe, Mn, Cr and Al, merely by selection of different photomultipliers in the spectrometer. After a number of improvements in the mechanical quality of the weld-chamber, and of the electronics, reproducible results have been obtained on National Bureau of Standards specimens. Presently, a set of standard signals is being assembled, after which actual welding alloys will be tested. If in the future, copper based, or aluminum based alloys are to be studied, the internal standard can be changed from iron to copper or aluminum.

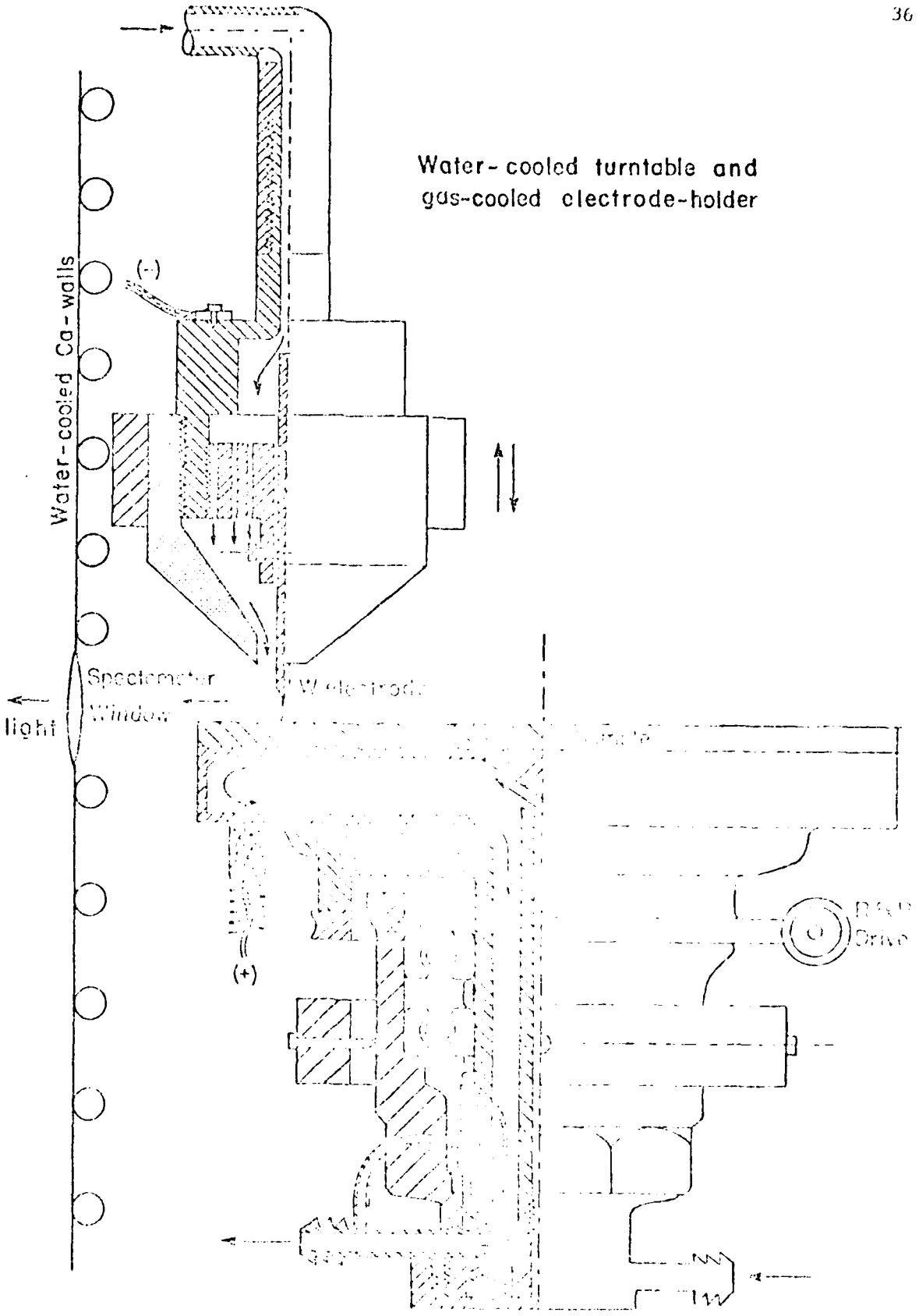
Water-cooled turntable and
gas-cooled electrode-holder
Water-cooled Ca-walls
(-)
Spectrometer
Window
light
(+)

Figure C-1

APPENDIX D

Ultrasonic Detection of the Weld Seam

Automatic welding can be considered to include at least two distinct aspects: the mechanization of the welding process, and control of the welding process to improve the quality and consistency of welded joints. A great deal of effort has been concentrated on the mechanization of welding; much less has been done to develop a means of controlling the weld quality itself.

Modern control theory is generally concerned with measuring the outputs of a system to be controlled, comparing them with a set of desired outputs, and then adjusting the inputs to the system in such a way that the desired outputs can be achieved. In the case of welding, the desired output is a joint between two metals that has the properties of a homogeneous piece of metal. Clearly, a welded joint can be inspected after welding in order to determine whether or not it is complete and can satisfactorily perform its function. However, if one is going to control the welding process, it will be necessary to find a set of parameters that can be measured during welding to provide an indication of the quality of a weld.

The welding parameter most commonly cited as being of potential value for determining the quality of a welded joint is the penetration. However, few techniques currently exist for measuring the penetration of a weld in-process. Such a technique would be of great value in implementing feedback control of welding.

In an effort to provide a means of measuring weld penetration, we are investigating the use of ultrasonic pulse-echo techniques. Ultrasonic inspection is commonly employed for the purpose of detecting flaws and inclusions in welded joints. A sound wave travelling through a medium will be reflected at locations where discontinuities or density gradients exist. Cracks, porosity,

APPENDIX D (continued)

and lack of fusion are examples of discontinuities in a welded joint which would reflect ultrasound.

Discontinuous density gradients will exist at the interface between solid and liquid metal and cause ultrasound to be reflected; hence, a molten weld puddle should reflect ultrasound. The manner in which ultrasound is reflected from a molten weld puddle and the amplitude of the reflected signal will be a function of the size and shape of the weld puddle. In principle one can determine the dimensions of a molten weld puddle from ultrasonic time trace data. The results of such measurements could then be used to decide how to alter arc current, torch travel speed, or other weld parameters in order to achieve the desired penetration.

The use of ultrasound for penetration measurement hinges on the ability to determine the size and shape of a

transmitted and received ultrasound signals. Perfecting the ability to do this is the major objective of current research in ultrasonic non-destructive testing. For the purposes of ultrasonic penetration measurement, two approaches to this measurement problem are being considered. The first is a geometrical ultrasonics approach that works under the assumption that ultrasound propagates in straight lines with narrow beamwidth. Under these conditions, the size and shape of a reflector can be determined from knowledge of the path followed by an ultrasound ray and the time it takes to travel that path. For smoothly curved surfaces with dimensions larger than the beamwidth, the geometrical ultrasonics approach should be quite practical. However, it is not at all clear that the problem of penetration measurement satisfies the constraints necessary to apply the geometric ultrasonics approach.

In the event that the geometric ultrasonics approach proves inadequate

for the purposes of penetration measurement, ultrasonic scattering techniques are being considered. In this approach ultrasound measurements are made in several locations and are used to estimate the size of a reflector from the distribution of the signals received at the different locations. Currently, several researchers are investigating frequency domain scattering techniques to determine the size of flaws in materials.

The current attempt to develop a system for the ultrasonic measurement and control of penetration can be broken down into three basic tasks: (1) verification of the concept of ultrasonic penetration measurement, (2) development of a practical technique for ultrasonic penetration measurement, and (3) development of weld penetration control concepts based on penetration measurement.

The first phase is presently underway and will consist of 2 sets of experiments, which will be used to evaluate the feasibility of ultrasonic penetration measurement. The first set of experiments will look at the capabilities of ultrasonic shape determination. Several curved surfaces have been milled into steel plate and will be examined with an ultrasonic probe. The ultrasound measurements and the equations of geometric ultrasonics will then be used to determine the size of the milled surface and the results will be compared with direct measurements to check their accuracy.

The second set of experiments will be performed to determine whether or not molten metal will adquately reflect ultrasound so that size measurements can be made. In order to perform these experiments a static molten puddle will be formed using a stationary TIG torch and an ultrasound transducer will be used to detect ultrasound reflections. If reflections can be detected, the next step will be to measure the size of the puddle from these reflections.

After the experiments are completed, the stationary welds will be sectioned and measured to see how well ultrasonic measurements of the puddle dimensions agree with the actual size of the solidified weld.

An ultrasound pulser receiver is currently under construction so that the above experiments can be carried out. Upon completion of the experiments the results will be examined and a decision reached about the viability and further development of the concept of ultrasonic penetration measurement.

Some preliminary experiments have been performed for both the "cold" and "hot" situations. The former indicated the expected reflections, but emphasized the need for well focused beams. The hot experiment was intended only to look for evidence of reflections from a molten region. By melting a spot on a plate with a stationary TIG torch and passing ultrasound through this region, new reflections were recorded that corresponded roughly to the molten region location. These experiments, therefore, give qualitative reinforcement to this measurement concept, and subsequent experiments will more precisely quantify these results.